

Dielectric Analysis of Microcapsule-Immobilized Composite Capsules Suspension: Substances Release

Wantong Li, Kongshuang Zhao,* Xiguang Chen, and Yang Li



Cite This: *Langmuir* 2020, 36, 966–971



Read Online

ACCESS |



Metrics & More

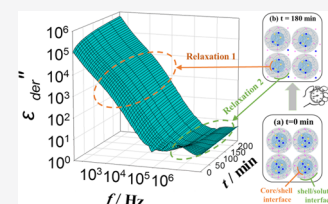


Article Recommendations



Supporting Information

ABSTRACT: Dielectric spectroscopy has unique advantages in monitoring drug release. In this work, a dielectric measurement was carried out on the release of the substances of microcapsule-immobilized composite capsules, which were fabricated by encapsulating the *Perinereis aibuhitensis* extract-loaded gum Arabic/gelatin microcapsules (PaE: GA/GE-MCs) in calcium alginate hydrogel (PaE: CA/GA/GE-CCs). We established the dielectric model of PaE: CA/GA/GE-CCs and got in-depth information on the systems. There are two relaxations in the dielectric spectroscopy, both of which are caused by interfacial polarization. The relaxation mechanisms correspond to the interfacial polarization of the PaE-loading core/calcium alginate shell interface and the calcium alginate shell/solution interface, respectively. Besides, the swelling of composite capsules and substance migration in the composite capsules were observed by analyzing phase parameters. Finally, the characteristic release of calcium alginate composite capsules was confirmed, and the substance release mechanism of composite capsules, namely, the swelling–diffusion mechanism, was obtained.



INTRODUCTION

Controlled release systems have attracted extensive attention in the last three decades.^{1,2} Ideal drug delivery vehicles are biocompatible and biodegradable; besides, drug release time and dose should be controlled at the same time. Alginate is a biocompatible material and can be tailor-made according to the actual application, so it has been applied to some of the controlled release systems such as the calcium alginate microsphere system, which can be used as a potential resveratrol delivery system in the food industry;³ a phosphate-alginate core–shell nanoparticle system, which is prepared for controlling gene and biomolecule entry into cell for therapy;⁴ multilayered alginate microcapsules for the sustained release of growth factor;⁵ and mineralized polysaccharide alginate membrane for sustained multiresponsive controlled drug delivery.⁶ These systems are all relatively simple alginate systems for common applications. To achieve more diversified functions, the researchers designed a system with microspheres embedded in calcium alginate gel beads as a dual drug delivery system to achieve the simultaneous encapsulation and release of hydrophilic and hydrophobic drugs.⁷

The system with microspheres embedded in calcium alginate gel beads can also be used to deliver oral enteric drugs for reducing the drug release amount in the stomach, which is based on the characteristic that calcium alginate shrinks in a strong acid environment and swells under neutral environment.^{8–10} However, the main disadvantage of alginate as a drug-controlled release carrier is the low drug encapsulation efficiency, especially for water-soluble drugs,² such as *Perinereis aibuhitensis* extract (PaE). PaE is a protein-rich, negatively charged hydrophilic mixture with strong antioxidant activity

and easy inactivation, so the delivery of PaE requires a suitable carrier. We used a special drug delivery system, the composite capsules, which were fabricated by encapsulating the PaE-loaded gum Arabic/gelatin microcapsules (PaE: GA/GE-MCs) in calcium alginate hydrogel (PaE: CA/GA/GE-CCs).¹¹ The PaE was absorbed on the shell of the microcapsules by electrostatic interaction,¹² and then the PaE-loaded microcapsules were embedded in the calcium alginate hydrogel. In this way, we achieved the purpose of protecting the antioxidant activity of PaE and at the same time increasing the encapsulation efficiency. This system has great potential in the oral enteric drug delivery, so it is necessary to understand the substance release process of PaE: CA/GA/GE-CCs from a theoretical point of view.

The release mechanism of the substances plays an important role in the release rate and release effect. The release mechanism of the alginate-based system includes diffusion, swelling, and erosion. In general, the release of a water-soluble drug is controlled by diffusion, while the water-insoluble drug is largely dependent on gel erosion for alginate-based drug delivery systems.^{13,14} However, it is not absolute. The nature and structure of drug release systems also have a significant influence on the release mechanism. Therefore, many researchers have studied the release process of the drug through different methods. For example, a mesoscopic simulation was used to study the drug release process,¹⁵ and

Received: November 13, 2019

Revised: January 14, 2020

Published: January 16, 2020

researches established the kinetics release model to predict drug release mechanisms.¹⁶ These methods can contribute to understand and develop drug delivery systems. Besides, dielectric relaxation spectroscopy (DRS) can also provide some unique information. Dielectric relaxation spectroscopy, which is sensitive to polarization processes including interfacial polarization and ion migration motion, has achieved great success in many areas including colloidal dispersions,^{17–19} which includes the drug release of microsphere suspensions; for example, real-time monitoring of the release process of salicylic acid release from chitosan gel beads by DRS.^{20,21}

In previous works, we have studied the drug release process of drug-loaded microspheres that have relatively simple structures.²⁰ In this work, we studied the drug-loaded multishell particle, whose structure is complicated, and it is necessary to establish the corresponding model for analysis. The substance release of PaE: CA/GA/GE-CCs in deionized water at room temperature was monitored by dielectric spectroscopy. The system, which is formed by adding the composite capsules into an aqueous solution, could be seen as a particle suspension based on the features of the system. Dielectric measurements and modeling of the PaE: CA/GA/GE-CCs suspension were performed to obtain information on the interface and substance migration in the release process and an insight into the possible release mechanism.

EXPERIMENTAL SECTION

Material and Sample Preparation. The preparation of PaE: CA/GA/GE-CCs: moderate PaE was dissolved in gum Arabic (GA) solution. Premelted stearic acid was mixed with gelatin solution to form uniform emulsified droplets and then mixed with PaE/GA solution and gelation by adding tannic acid to obtain PaE: GA/GE-MCs. The obtained PaE: GA/GE-MCs were mixed with sodium alginate (SA) solution, and the microcapsules were uniformly dispersed in the solution. The mixed solution was dropped into a CaCl₂ solution with a syringe to finally form PaE: CA/GA/GE-CCs. The lyophilized PaE: CA/GA/GE-CCs were spherical and uniform, with a particle size of 1.35 ± 0.16 mm. The detailed preparation process is described in ref 11.

PaE: CA/GA/GE-CCs were mixed with deionized water to form the PaE: CA/GA/GE-CC suspension.

Dielectric Measurements. Dielectric measurement of the PaE: CA/GA/GE-CC suspension was carried out by an HP4294A precision impedance analyzer (Agilent Technologies) at 40 Hz to 110 MHz. The applied ac electric field was 500 mV, and all of the samples were measured at 25 °C. The measuring cell used in the test for the case of PaE: CA/GA/GE-CCs suspension is a parallel plate capacitor of platinum disks and separated by a Lucite spacer. However, the measured original data (capacitance C_x and conductance G_x) contain the influence of the measuring cell; therefore, the original data obtained needs to be corrected. First, the cell constant ($C_1 = 0.0554$ pF), stray capacitance ($C_r = 0.525$ pF), and residual inductance ($L_r = 4.58 \times 10^{-7}$ F/S²) of the cell were calibrated with standard substances (air, ethanol, and pure water), and then the original data were corrected according to the Schwan method²²

$$C_s = \frac{C_x(1 + \omega^2 L_r C_x) + L_r G_x^2}{(1 + \omega^2 L_r C_x)^2 + (\omega L_r G_x)^2} - C_r \quad (1)$$

$$G_s = \frac{G_x}{(1 + \omega^2 L_r C_x)^2 + (\omega L_r G_x)^2} \quad (2)$$

where $\omega (=2\pi f)$, f is the frequency) is the angular frequency. The subscripts x and s represent the actual measured data and the corrected data, respectively. Then, permittivity ϵ and conductivity κ of the sample are obtained after the conversion using the formula: $\epsilon =$

$(C_s - C_r)/C_b$, $\kappa = G_s \epsilon_0 / C_1$ ($\epsilon_0 = 8.8541 \times 10^{-12}$ F/m, vacuum permittivity).

Determination of Dielectric Parameters. Under the ac electric field, the dielectric properties of PaE: CA/GA/GE-CC suspension can be expressed by the complex permittivity $\epsilon^*(\omega)$

$$\epsilon^*(\omega) = \epsilon' - j\epsilon'' = \epsilon - j \frac{\kappa(\omega)}{\omega \epsilon_0} \quad (3)$$

where $\epsilon'(\omega)$ and $\epsilon''(\omega)$ are the real and imaginary parts of ϵ^* , respectively, and $j = (-1)^{1/2}$. A considerable electrode polarization (EP) occurred in the low frequency (LF) of dielectric spectroscopy. The EP obscures the LF relaxation; to separate the contribution of EP, Cole–Cole equation²³ (eq 4) with the electrode polarization term $A\omega^{-m}$ (A and m are adjustable parameters) was employed to analyze the dielectric spectroscopy.

$$\epsilon^* = \epsilon_h + \sum_i \frac{\Delta \epsilon_i}{1 + (j\omega\tau_i)^{\beta_i}} + A\omega^{-m} \quad (4)$$

where i refers to the i th relaxation, so its value indicates the number of relaxations; ϵ_h and $\epsilon_l (= \epsilon_h + \sum \Delta \epsilon_i)$ are high- and low-frequency limits of permittivity, respectively. β_i ($0 < \beta_i \leq 1$) is the Cole–Cole parameter indicating the distribution of the relaxation time. The curve fitting of the Cole–Cole equation without the EP term was carried out by the Levenberg–Marquardt method to minimize the sum of the residuals of the real and imaginary parts of complex permittivity, that is, $\chi = \sum_i [e'_e(\omega_i) - e'_t(\omega_i)]^2 + \sum_i [e''_e(\omega_i) - e''_t(\omega_i)]^2$, where subscripts e and t , respectively, refer to experimental and theoretical values.²⁴

Therefore, we removed the influence of electrode polarization on ϵ and obtained the frequency dependence of ϵ removed EP of PaE: GA/GE-CC suspension at different times (Figure 1a). Besides, eq 4

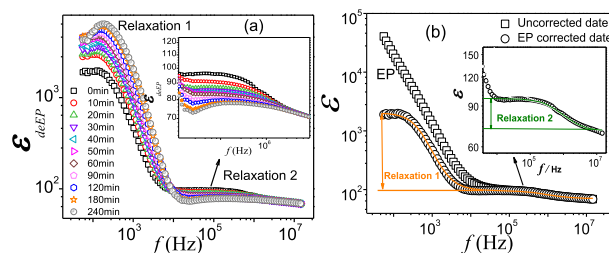


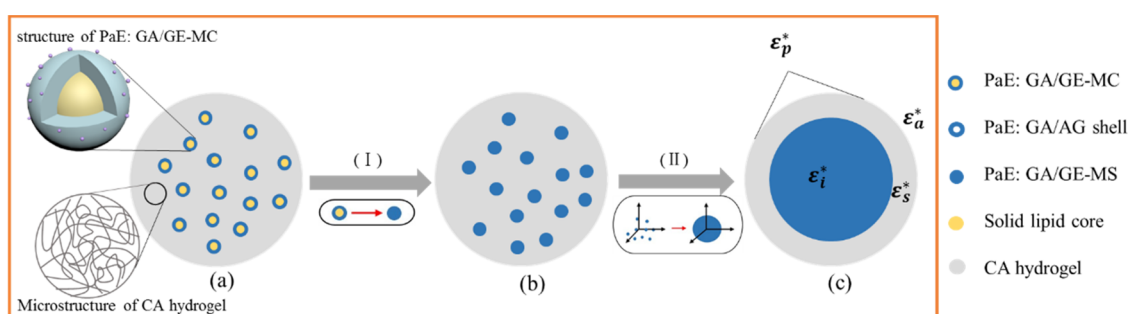
Figure 1. (a) Relationship between permittivity ϵ and frequency f of PaE: GA/GE-CC suspension at $t = 0$ min. The inset shows the enlarged view of relaxation 2 (solid lines are the best fitting line). (b) The frequency dependence of ϵ without EP of PaE: GA/GE-CC suspension at different times.

without the EP term was used to fit the $\epsilon_{\text{deEP}} - f$ data; an example is shown in Figure 1b. Based on the best fitting results, relaxation time $\tau_i (=1/2\pi f_{0i})$ where f_0 is the characteristic relaxation frequency) and dielectric increment $\Delta \epsilon_i$ were obtained and the results are listed in Table 1. The above parameters, including f_{0i} , $\Delta \epsilon_i$, ϵ_{hi} , ϵ_{li} , τ_{pi} and β_i are all named dielectric parameters.

Modeling of Microcapsule-Immobilized Composite Capsules. The dielectric modeling analysis is necessary for this system. Figure 2 shows the modeling of composite capsules. The modeling dielectric analysis started by establishing the dielectric model. First, as shown in Figure 2I, the core–shell structure of PaE: GA/GE-MCs is simplified and approximated as a PaE-loaded gum Arabic/gelatin microspheres (PaE: GA/GE-MSs) because solid–lipid cores of PaE: GA/GE-MCs have little effect on the release of PaE. Based on the above premise, the model of PaE: CA/GA/GE-CCs is simplified from Figure 2a (this structure was verified by Figure S3b of the Supporting Information) to Figure 2b. Second, all of the small PaE: GA/GE-MSs within a calcium alginate capsule are assembled into one large microsphere as shown in Figure 2II, which is reasonable based on the fact that interface problem is mainly involved in this work and

Table 1. Dielectric Parameters of PaE: CA/GA/GE-CC Suspension Calculated by the Cole–Cole Equation

t/min	ϵ_i	$\Delta\epsilon_1$	$\Delta\epsilon_2$	f_1/Hz	$f_2/10^5 \text{ Hz}$
0	69.92 ± 0.09	1979 ± 7	25.87 ± 0.09	453.1 ± 0.4	8.596 ± 0.018
10	69.68 ± 0.07	3007 ± 11	21.00 ± 0.07	464.0 ± 0.9	12.69 ± 0.09
20	70.05 ± 0.12	3250 ± 10	17.32 ± 0.10	505.8 ± 0.6	13.66 ± 0.15
30	70.35 ± 0.11	3650 ± 8	15.72 ± 0.12	522.2 ± 0.8	13.90 ± 0.11
40	70.63 ± 0.16	4017 ± 9	14.17 ± 0.06	549.7 ± 1.1	14.20 ± 0.19
50	70.77 ± 0.12	4505 ± 11	13.23 ± 0.04	568.9 ± 0.9	14.29 ± 0.12
60	70.80 ± 0.08	4828 ± 12	12.51 ± 0.05	571.2 ± 1.3	14.30 ± 0.17
90	70.88 ± 0.05	5113 ± 15	10.61 ± 0.09	597.0 ± 1.2	14.82 ± 0.15
120	70.82 ± 0.07	5367 ± 13	9.676 ± 0.025	651.2 ± 2.1	16.79 ± 0.23
180	70.80 ± 0.15	5582 ± 14	8.534 ± 0.021	710.8 ± 2.2	17.64 ± 0.18
240	70.32 ± 0.14	5757 ± 15	8.428 ± 0.023	761.4 ± 3.1	20.88 ± 0.24

**Figure 2.** Modeling of composite capsules. (a) Actual model of PaE: CA/GA/GE-CCs. (b, c) Simplified model of PaE: CA/GA/GE-CCs after first and the second simplification, respectively. (I, II) First and the second steps for simplification, respectively. (c) is used to describe the structure of a composite capsule in the following text.**Table 2. Phase Parameters of PaE: CA/GA/GE-CCs Suspension Calculated by the Hanai Analytical Method**

t/min	ϕ	$\kappa_2 \text{ (mS/m)}$	ϵ_i	$\kappa_1 \text{ (S/m)}$
0	0.7493 ± 0.0015	24.78 ± 0.12	58.39 ± 0.25	0.08574 ± 0.00035
10	0.7431 ± 0.0013	28.49 ± 0.17	50.26 ± 0.24	0.1157 ± 0.0009
20	0.7380 ± 0.0011	31.01 ± 0.19	50.08 ± 0.26	0.1628 ± 0.0011
30	0.7362 ± 0.0014	33.36 ± 0.15	52.92 ± 0.31	0.2074 ± 0.0013
40	0.7345 ± 0.0018	35.38 ± 0.13	55.92 ± 0.23	0.2645 ± 0.0012
50	0.7339 ± 0.0010	37.15 ± 0.14	57.67 ± 0.19	0.3133 ± 0.0015
60	0.7329 ± 0.0019	38.40 ± 0.18	56.95 ± 0.25	0.3501 ± 0.0014
90	0.7294 ± 0.0015	42.12 ± 0.20	54.19 ± 0.21	0.4908 ± 0.0017
120	0.7279 ± 0.0012	45.39 ± 0.22	47.84 ± 0.17	0.5926 ± 0.0016
180	0.7258 ± 0.0017	49.87 ± 0.23	39.01 ± 0.19	0.7807 ± 0.0019

interfacial environment of each PaE: GA/GE-MS is uniform. As a result, PaE: CA/GA/GE-CC is approximated as a core–shell capsule (Figure 2c) after two-step simplification, where PaE: GA/GE-MS is the core and calcium alginate gel is the shell. Besides, the reasonability of the model in Figure 2c was proved by simulation in Section 2 of the Supporting Information. The simulation results are consistent with the experimental results, that is, two relaxations observed in the simulation results and the changing trends of the relaxation parameters of two relaxations are consistent with the experimental results in the $\epsilon-f$ plot and $\kappa-f$ plot.

RESULTS AND DISCUSSION

Relaxation Mechanism of PaE: CA/GA/GE-CCs Suspension. There are two relaxations (relaxation 1 and relaxation 2) located in the frequency range of 4×10^2 to 2×10^7 Hz in Figure 1a. Based on our experiences with the core–shell particle dispersion systems, the relaxation mechanism in this frequency range is usually the interfacial polarization.^{18,25,26} It is interesting that two interfaces exactly exist in the PaE: CA/GA/GE-CC suspension system, and they

are the interface of the PaE: GA/GE-MS core/calcium alginate (CA) shell and the interface of the CA shell/aqueous solution. Two interfaces correspond to two relaxations, respectively. The relaxation, which is induced by the interface of alginate/ aqueous, is located around 10^{-7} s in general,^{27,28} consistent with relaxation 2 of the PaE: CA/GA/GE-CC suspension in this work. It was concluded that relaxation 2 is derived from the interfacial polarization of the alginate/ aqueous solution interface. In this premise, it was also logical that relaxation 1 is induced by the interfacial polarization of the interface of PaE: GA/GE-MS core and CA shell.

Calculation of Phase Parameters of PaE: CA/GA/GE-CC Suspension. The system, which is PaE: CA/GA/GE-CCs dispersed in aqueous solution, can be approximately modeled as a core–shell particle suspension: particles having a complex permittivity ϵ_p^* dispersed in a medium having a complex permittivity ϵ_a^* with volume fraction ϕ as shown in Figure 2c. Equation 5 is the formula of the equivalent complex permittivity of the core–shell particles. Substituting eq 5 into

the Hanai equation (eq 6), we obtain the general compression of the complex permittivity of the core–shell spherical particle suspension. Then, the corresponding Hanai analytical method^{29,30} was used to obtain phase parameters (ϕ , ε_p , κ_i , κ_a , ε_p , ε_a , κ_s) of the PaE: CA/GA/GE-CC suspension by calculating the dielectric parameters. The results are shown in Table 2.

$$\varepsilon_p^* = \varepsilon_s^* \frac{2(1-\nu)\varepsilon_s^* + (1+2\nu)\varepsilon_i^*}{(2+\nu)\varepsilon_s^* + (1-\nu)\varepsilon_i^*} \quad (5)$$

$$\left(\frac{\varepsilon_a^* - \varepsilon_p^*}{\varepsilon_a^* - \varepsilon_s^*} \right) \left(\frac{\varepsilon_s^*}{\varepsilon_i^*} \right)^{1/3} = 1 - \phi \quad (6)$$

where $\varepsilon_s^* (= \varepsilon_s + \kappa_s/(j\omega\varepsilon_0))$ and $\varepsilon_i^* (= \varepsilon_i + \kappa_i/(j\omega\varepsilon_0))$ are the complex permittivity of the shell and core phases of the capsules, respectively. ν is the volume ratio of the core to the core–shell capsules. ε_m and ε_l are the permittivities of the middle and low frequencies, respectively. κ_m and κ_l are the conductivities of the middle and low frequencies, respectively.

Swelling of PaE: CA/GA/GE-CCs. The shell thickness d_s of PaE: CA/GA/GE-CCs at different times is shown in Figure 3. The values of d_s were calculated by the Hanai analytical

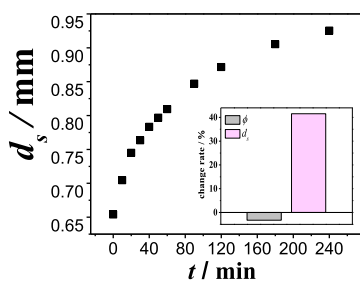


Figure 3. Time dependence of the shell thickness d_s of PaE: CA/GA/GE-CCs. The inset shows the change rate of the value of d_s and ϕ from 0 to 240 min.

method. It is obvious that d_s increases as the measurement time increases because the calcium alginate shell swells with the absorbing of water due to the hydration of hydrophilic groups in the neutral media.^{31,32} If no other reaction occurs in the system at this moment, then the volume fraction ϕ of the composite capsules should also increase with the increasing shell thickness d_s . However, the change rate of ϕ is not only negative but also small compared with d_s , which can be seen in the inset of Figure 3. Equation 7 is the formula of ϕ . V_T and V_c are the volumes of the total system and capsules, respectively; R and N are the radius of the core and the number of capsules, respectively. During the experiment, the measuring cell was closed and there were no substances in and out, and V_T is a constant. At the same time, because the composite capsule is in the millimeter scale and visible to the naked eye, in the short measurement process, we observed that the number of capsules does not change; therefore, N was considered as a constant. In the premise that V_T and N are constant, ϕ is proportional to R and d_s . Therefore, it means that the value of R decreases when d_s increases and ϕ decreases.

$$\phi = \frac{V_c}{V_T} = \frac{N(R + d_s)^3}{V_T} \quad (7)$$

The change in the interaction between PaE and other materials plays an important role in this situation. PaE is a hydrophilic mixture and attaches to the PaE: GA/GE-MS core depending strongly on the electrostatic force and van der Waals force.³³ However, PaE bonds with water through hydrogen bonds when PaE meets aqueous solution. The water content of the shell increases when measurements are conducted; it is reasonable to conclude that a part of PaE tends to destroy the original van der Waals force, bonds with water and enters the aqueous solution because van der Waals force is weaker than the hydrogen bond. Therefore, we speculated that PaE with water in the PaE: GA/GE-MS core expels out of the core, which causes the shrinkage of the core. This is the reason why d_s increases but ϕ almost remains constant.

Substance Release Mechanism of PaE: CA/GA/GE-CCs. Substance Migration in the PaE: CA/GA/GE-CC Suspension. Figure 4 shows the solution phase conductivity

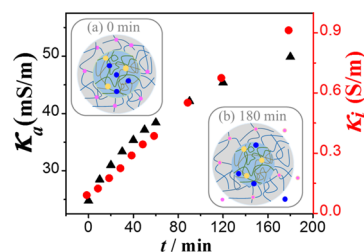


Figure 4. Solution phase conductivity κ_a and core phase conductivity κ_i at different times. The state of PaE: CA/GA/GE-CCs at (a) 0 min and (b) 180 min. In the inset, the small pink, yellow, and blue circles represent Ca^{2+} , PaE attached to the cores by electrostatic force, and PaE attached to the core by van der Waals force, respectively.

κ_a and core phase conductivity κ_i at different times. Inset of (a) and (b) in Figure 4 show the states of PaE: CA/GA/GE-CCs at 0 and 180 min, respectively. We can notice that the solution phase conductivity κ_a and core phase conductivity κ_i both increase with increasing time. The reasons for the increase are different from each other. For κ_a , two substances should be taken into account, that is, the free Ca^{2+} and charged PaE migrate into the solution, which we discussed above. On the other hand, the increase of κ_i is induced by other reasons. The increase of κ_i is caused by the increase of free charges in the core. A part of PaE, which attached to the cores of PaE: CA/GA/GE-CCs by van der Waals forces, is gradually desorbed when PaE: CA/GA/GE-CCs are located in the solution. As the measurement time increases, the electrostatic interaction between gelatin, gum Arabic, and PaE is gradually destroyed, the hydrophilic PaE is gradually desorbed in the cores, and free charged ions are accumulated in the cores. These are the reasons why κ_i increasing. The inset of Figure 4a,b clearly shows the process of substance migration in the suspension system.

Release Characteristic of PaE: CA/GA/GE-CCs. Figure 5a,b shows the dielectric parameters ($\Delta\varepsilon$ and τ) vs time plot of relaxation 1 and relaxation 2, respectively. It should be noticed that the trend is fast and then slow no matter which parameter changes with time in Figure 5. We concluded that this phenomenon is an explosive release,^{31,34} which is a characteristic release mode when calcium alginate gel is used as a drug delivery carrier because of the porous structure of calcium alginate gel.

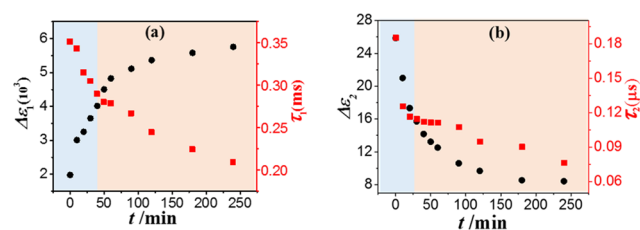


Figure 5. Time dependence of $\Delta\epsilon$ and τ of (a) relaxation 1 and (b) relaxation 2.

The values of dielectric increment $\Delta\epsilon_1$ increase while the values of relaxation time τ_1 decrease as the time increases, as shown in Figure 5a. However, the values of both $\Delta\epsilon_2$ and τ_2 of relaxation 2 decrease in Figure 5b. This indicates that the relaxations 1 and 2 were induced by different reasons. Both relaxations 1 and 2, which have been discussed here, are derived from interfacial polarization. The dielectric increment is related to the difference of electrical properties between the dispersed phase and the medium phase in the interface polarization theory.³⁵ The relaxation time is dependent on the response time of the system to the electric field.

Although relaxations 1 and 2 are both derived from interfacial polarization, the characteristics of two relaxations are greatly different. Besides, the effect of the medium phase on the two relaxations is also different. Relaxation 1 is caused by the interfacial polarization of the core/CA shell interface. After PaE: CA/GA/GE-CCs are placed in aqueous solution, a part of PaE, which is attached to the core by van der Waals force, tends to desorb from the core and enter into aqueous solution. At this time, PaE, moved more freely and oriented faster because it was desorbed and charged. It is reasonable that the interface charge can reach the equilibrium more quickly under an applied ac electric field, resulting in a decrease of the value of τ_1 . However, charged PaE is limited to the CA gel three-dimensional network so that the PaE migration is difficult and PaE is accumulated initially on the surface of the core, leading to the increase in the difference of electrical properties between two phases (PaE: GA/GE-MS core phase and CA shell phase). As a result, $\Delta\epsilon_1$ increases.

Relaxation 2 is caused by the interfacial polarization of the CA shell/solution interface. The reason for the decrease of τ_2 is different from τ_1 . As the measurement time increases, CA gel absorbs water, and the three-dimensional network swells, the extent of space limitation of interface charges is reduced. Under the applied electric field, the motion is freer and the orientation speed of the interface charge is faster, which reduces the time required to reach an equilibrium. Therefore, τ_2 decreases. At the same time, there are a large number of free ions in the CA gel phase, such as free Ca^{2+} . Ca^{2+} in the CA gel phase gradually diffuses into the solution due to the concentration difference, leading to a reduction in the difference between electrical properties of the CA gel phase and those of the aqueous phase; therefore, $\Delta\epsilon_2$ decreases.

CONCLUSIONS

This work measured the dielectric spectroscopy of the microcapsule-immobilized composite capsules suspension and discussed the substance release of composite capsules based on modeling. After subtracting the influence of electrode polarization, two relaxations were found in the low and high frequencies of dielectric spectroscopy, which were caused by the interfacial polarization of the interface of the PaE: GA/GE-

CC core/CA shell and the interface of the CA shell/medium, respectively. Besides, we observed the swelling of capsules and substance migration in the suspension by analyzing the phase parameters. Meanwhile, the changes of various parameters proved that there was explosive drug release. Finally, the drug release mechanism of PaE: CA/GA/GE-CCs was obtained, that is, the swelling–diffusion mechanism. We obtained the internal information of the microcapsule-immobilized composite capsules suspensions by dielectric spectroscopy method and analyzed the substance release of PaE: CA/GA/GE-CCs from the mathematical point of view, which provided a reference for further utilization of microcapsule-immobilized composite capsule.

ASSOCIATED CONTENT

Supporting Information

The Supporting Information is available free of charge at <https://pubs.acs.org/doi/10.1021/acs.langmuir.9b03539>.

Simulation of dielectric behavior of the core–shell particle suspension and sample characterization (PDF)

AUTHOR INFORMATION

Corresponding Author

Kongshuang Zhao – College of Chemistry, Beijing Normal University, Beijing 100875, China; orcid.org/0000-0001-5863-2017; Email: zhaoks@bnu.edu.cn

Authors

Wantong Li – College of Chemistry, Beijing Normal University, Beijing 100875, China

Xiguang Chen – Biochemistry and Biomaterial Key Laboratory of Shandong Colleges and Universities, College of Marine Life Science, Ocean University of China, Qingdao 266003, China

Yang Li – Biochemistry and Biomaterial Key Laboratory of Shandong Colleges and Universities, College of Marine Life Science, Ocean University of China, Qingdao 266003, China

Complete contact information is available at:

<https://pubs.acs.org/10.1021/acs.langmuir.9b03539>

Notes

The authors declare no competing financial interest.

ACKNOWLEDGMENTS

Financial support for this work from the National Natural Science Foundation of China (Grants 21673002 and 21473012) is gratefully acknowledged.

ABBREVIATIONS

PaE	<i>Perinereis aibuhitensis</i> extract
GA/GE-MCs	gum Arabic/gelatin microcapsules
PaE: GA/GE-MCs	PaE-loaded gum Arabic/gelatin microcapsules
PaE: GA/GE-MSs	PaE-loaded gum Arabic/gelatin microspheres
CA/GA/GE-CCs	calcium alginate/gum Arabic/gelatin composite capsules
PaE: CA/GA/GE-CCs	PaE-encapsulated CA/GA/GE-CCs

REFERENCES

- (1) Zhang, Y.; Chan, H. F.; Leong, K. W. Advanced materials and processing for drug delivery: The past and the future. *Adv. Drug Delivery Rev.* **2013**, *65*, 104–120.

- (2) Tapan Kumar, G.; Deepa, T.; Amit, A.; Hemant, B.; Dulal Krishna, T. Alginate based hydrogel as a potential biopolymeric carrier for drug delivery and cell delivery systems: present status and applications. *Curr. Drug Delivery* **2012**, *9*, 539–555.
- (3) Cho, A. R.; Yong, G. C.; Kim, B. K.; Dong, J. P. Preparation of alginate–CaCl₂ microspheres as resveratrol carriers. *J. Mater. Sci.* **2014**, *49*, 4612–4619.
- (4) Ahn, G.; Yu, G.; Abdullah, A.; Kim, Y.; Lee, D. Controlling the Release Profile Through Phase Control of Calcium Phosphate-Alginate Core-shell Nanoparticles in Gene Delivery. *Macromol. Res.* **2019**, *27*, 579–585.
- (5) Omadiya, K.; Moya, M. L.; Opara, E. C.; Brey, E. M. Synthesis of multilayered alginate microcapsules for the sustained release of fibroblast growth factor-1. *J. Biomed. Mater. Res., Part A* **2010**, *95A*, 632–640.
- (6) Shi, J.; Liu, X.; Shang, Y.; Cao, S. Biomineralized polysaccharide alginate membrane for multi-responsive controlled drug delivery. *J. Membr. Sci.* **2010**, *352*, 262–270.
- (7) Zhong, D.; Liu, Z.; Xie, S.; Zhang, W.; Zhang, Y.; Xue, W. Study on poly (D,L-lactic) microspheres embedded in calcium alginate hydrogel beads as dual drug delivery systems. *J. Appl. Polym. Sci.* **2013**, *129*, 767–772.
- (8) Hwang, S. J.; Rhee, G. J.; Lee, K. M.; Oh, K. H.; Kim, C. K. Release characteristics of ibuprofen from excipient-loaded alginate gel beads. *Int. J. Pharm.* **1995**, *116*, 125–128.
- (9) Yotsuyanagi, T.; Ohkubo, T.; Ohhashi, T.; Ikeda, K. Calcium-induced gelation of alginate acid and pH-sensitive reswelling of dried gels. *Chem. Pharm. Bull.* **1987**, *35*, 1555–1563.
- (10) González-Rodríguez, M. L.; Holgado, M. A.; Sánchez-Lafuente, C.; Rabasco, A. M.; Fini, A. Alginate/chitosan particulate systems for sodium diclofenac release. *Int. J. Pharm.* **2002**, *232*, 225–234.
- (11) Li, Y.; Liang, M.; Dou, X.; Feng, C.; Pang, J.; Cheng, X.; Liu, H.; Liu, T.; Wang, Y.; Chen, X. Development of alginate hydrogel/gum Arabic/gelatin based composite capsules and their application as oral delivery carriers for antioxidant. *Int. J. Biol. Macromol.* **2019**, *132*, 1090–1097.
- (12) Pakulska, M. M.; Donaghue, I. E.; Obermeyer, J. M.; Tuladhar, A.; McLaughlin, C. K.; Shendruk, T. N.; Shoichet, M. S. Encapsulation-free controlled release: Electrostatic adsorption eliminates the need for protein encapsulation in PLGA nanoparticles. *Sci. Adv.* **2016**, *2*, No. e1600519.
- (13) Goh, C. H.; Heng, P. W. S.; Chan, L. W. Alginates as a useful natural polymer for microencapsulation and therapeutic applications. *Carbohydr. Polym.* **2012**, *88*, 1–12.
- (14) Sriamornsak, P.; Thirawong, N.; Korkerd, K. Swelling, erosion and release behavior of alginate-based matrix tablets. *Eur. J. Pharm. Biopharm.* **2007**, *66*, 435–450.
- (15) Rodríguez-Hidalgo, M. D. R.; Soto-Figueroa, C.; Vicente, L. Mesoscopic simulation of the drug release mechanism on the polymeric vehicle P(ST-DVB) in an acid environment. *Soft Matter* **2011**, *7*, 8224–8230.
- (16) Dash, S.; Murthy, P. N.; Nath, L.; Chowdhury, P. Kinetic Modeling on Drug Release from Controlled Drug Delivery Systems. *Acta Pol. Pharm.* **2010**, *67*, 217–223.
- (17) Cametti, C.; Fratoddi, I.; Venditti, I.; Russo, M. V. Dielectric relaxations of ionic thiol-coated noble metal nanoparticles in aqueous solutions: electrical characterization of the interface. *Langmuir* **2011**, *27*, 7084.
- (18) Su, W.; Man, Y.; Zhao, K.; Ngai, T. Influence of Charged Groups on the Structure of Microgel and Volume Phase Transition by Dielectric Analysis. *Macromolecules* **2016**, *49*, 7997–8008.
- (19) Masci, G.; Ladogana, R. D.; Cametti, C. Assemblies of thermoresponsive diblock copolymers: micelle and vesicle formation investigated by means of dielectric relaxation spectroscopy. *J. Phys. Chem. B* **2012**, *116*, 2121–2130.
- (20) Fang, M.; Gao, J. L.; Wang, S.; Lian, Y. W.; Zhao, K. S. Dielectric monitoring method for the drug release mechanism of drug-loading chitosan microspheres. *Chin. Sci. Bull.* **2010**, *55*, 1246–1254.
- (21) Chen, Z.; Ni, N.; Zhao, K. Real-time monitor on the release of salicylic acid from chitosan gel beads by means of dielectric spectroscopy. *Colloid Polym. Sci.* **2010**, *288*, 1245–1253.
- (22) Schwan, H. P. *Electrophysiological Methods*; William, L. N., Ed.; Academic: New York, 1963; Vol. 8, pp 323–407.
- (23) Cole, K. S.; Cole, R. H. Dispersion and Absorption in Dielectrics I. Alternating Current Characteristics. *J. Chem. Phys.* **1941**, *9*, 341–351.
- (24) Asami, K. Dielectric relaxation in a water-Oil-triton X-100 microemulsion near phase inversion. *Langmuir* **2005**, *21*, 9032–9037.
- (25) Wu, H.; Zhao, K. Dielectric Relaxation of Spherical Polyelectrolyte Brushes: Movement of Counterions and Electrical Properties of the Brush Layer. *Langmuir* **2015**, *31*, 8566–8576.
- (26) Guo, X.; Zhao, K. Dielectric Analysis based on Spherical-Shell Model for Cationic and Anionic Spherical Polyelectrolyte Brushes. *J. Phys.: Condens. Matter* **2017**, *29*, No. 29S101.
- (27) Esch, M.; Sukhorukov, V. L.; Kürschner, M.; Zimmermann, U. Dielectric properties of alginate beads and bound water relaxation studied by electrorotation. *Biopolymers* **2015**, *50*, 227–237.
- (28) Allgén, L. G.; Roswall, S. A dielectric study of sodium alginate in aqueous solution. *J. Polym. Sci.* **2010**, *23*, 636–650.
- (29) Hanai, T. *Electric Properties of Emulsions*; Academic Press: New York, 1968.
- (30) Zhang, H. Z.; Sekine, K.; Hanai, T.; Koizumi, N. Dielectric approach to polystyrene microcapsule analysis and the application to the capsule permeability to potassium chloride. *Colloid Polym. Sci.* **1984**, *262*, 513–520.
- (31) Pasparakis, G.; Bouropoulos, N. Swelling studies and in vitro release of verapamil from calcium alginate and calcium alginate–chitosan beads. *Int. J. Pharm.* **2006**, *323*, 34–42.
- (32) Lupo, B.; Maestro, A.; Gutiérrez, J. M.; González, C. Characterization of alginate beads with encapsulated cocoa extract to prepare functional food: Comparison of two gelation mechanisms. *Food Hydrocolloids* **2015**, *49*, 25–34.
- (33) Chesko, J.; Kazzaz, J.; Ugozzoli, M.; O'Hagan, D. T.; Singh, M. An investigation of the factors controlling the adsorption of protein antigens to anionic PLG microparticles. *J. Pharm. Sci.* **2005**, *94*, 2510–2519.
- (34) Li, J.; Su, Y. K.; Chen, X.; Park, H. J. Calcium-alginate beads loaded with gallic acid: Preparation and characterization. *LWT–Food Sci. Technol.* **2016**, *68*, 667–673.
- (35) Takashima, S. *Electrical Properties of Biopolymers and Membranes*; Adam Hilger: Bristol, 1989.